Electronic Supplementary Information

Selective recognition of choline phosphate by tripodal hexa-urea receptors with dual binding sites: crystal and solution evidence

Wei Zuo,[#] Chuandong Jia,[#] Huizheng Zhang, Yanxia Zhao, Xiao-Juan Yang,* and Biao Wu*

Key Laboratory of Synthetic and Natural Functional Molecule Chemistry of the Ministry of Education, College of Chemistry and Materials Science, Northwest University, Xi'an 710127, China

---

Table of Contents:

S1. General considerations

All reagents were obtained commercially and used without further purification. All NMR spectra were obtained at 20 ℃ by using Bruker AVANCE III-400 MHz spectrometers. ^{1}H and ^{13}C NMR chemical shifts were reported relative to residual solvent peaks (^{1}H NMR: 2.50 ppm for [D_6]DMSO; ^{13}C NMR: 39.52 ppm for [D_6]DMSO). Infrared (IR) spectra were recorded on a Bruker EQUIOX-55 spectrometer. Mass spectra

of ligand $\mathbf{L^2}$ and complexes **1**−**3** were measured with a Bruker micrOTOF-Q II ESI-Q-TOF LC/MS/MS spectrometer. Melting points were detected on an X-4 Digital Vision MP instrument. Fluorescence spectra were measured on a Horiba FL1039A/40A spectrophotometer in a 1 cm quartz cell.

S2. Synthesis of $\mathbf{L^2}$ and complexes 1−3

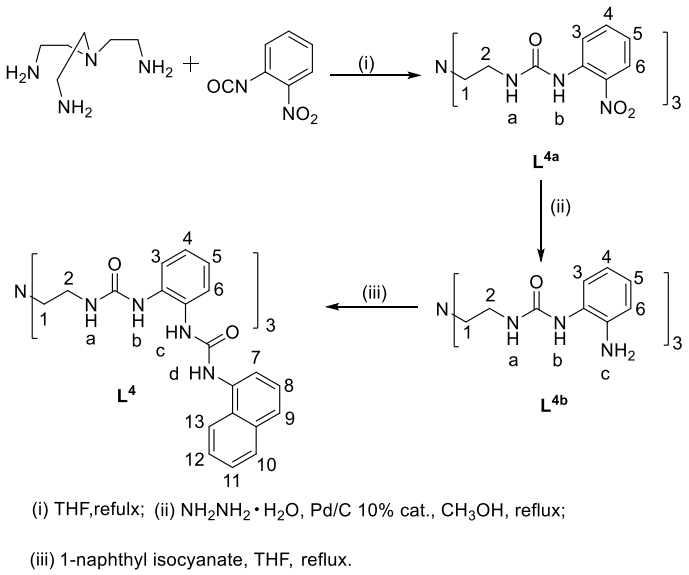

Scheme S1. Synthesis of the ligand $\mathbf{L^2}$.

$\mathbf{L^{2a}}$: Compound $\mathbf{L^{2a}}$ was prepared according to reported literature procedures.[1] ^{1}H NMR (400 MHz, [D_6]DMSO, ppm): δ 9.37 (s, 3H, NHb), 8.24 (d, J = 8.0 Hz, 3H, H6), 8.00 (d, J = 8.0 Hz, 3H, H3), 7.58 (t, J = 8.0 Hz, 3H, H4), 7.47 (s, 3H, NHa), 7.08 (t, J = 5.0 Hz, 3H, H5), 3.21 (m, 6H, H2), 2.64 (t, J = 6.4 Hz, 6H, H1).

$\mathbf{L^{2b}}$: Compound $\mathbf{L^{2b}}$ was prepared according to reported literature procedures.[1] ^{1}H NMR (400 MHz, [D_6]DMSO, ppm): δ 7.61 (s, 3H, Hb), 7.21 (d, J = 8.0 Hz, 3H H3), 6.78 (t, J = 8.0 Hz, 3H, H5), 6.68 (d, 3H, J = 8.0 Hz, H6), 6.50 (t, J = 8.0 Hz, 3H, H4), 6.21 (t, J = 5.4 Hz, 3H, Ha), 4.70 (s, 6H, Hc), 3.17 (m, 6H, H2), 2.57 (t, J = 6.4 Hz, 6H, H1).

Ligand $\mathbf{L^2}$: $\mathbf{L^{2b}}$ (0.5 g, 0.91 mmol) was added to a solution (4 mL DMF/20 mL THF) of 1-naphthyl isocyanate (0.51 g, 3.0 mmol). The mixture was refluxed over night and the precipitate thus obtained was filtered off and washed with THF and diethyl ether and then dried over vacuum to yield a white solid (0.84 g, 87%). M.p. 195 ℃. ^{1}H NMR (400 MHz, [D_6]DMSO, ppm): δ 9.10 (s, 3H, NHd), 8.44(s, 3H, NHc), 8.15 (d, J = 8.0 Hz, 3H, H13), 7.98 (d, J = 8.0 Hz, 3H, H7), 7.97 (s, 3H, NHb), 7.91 (d, J = 8.0 Hz, 3H, H10), 7.61 (m, 6H, H6 + H9), 7.43-7.57 (m, 12H, H3 + H8 + H11 +H12), 7.00 (m, 6H, H4 + H5), 6.54 (t, J = 5.0 Hz, 3H, NHa), 3.20 (m, 6H, H2), 2.61 (t, J = 6.8 Hz, 6H, H1). ^{13}C NMR (100 MHz, [D_6]DMSO): 156.1,

153.7, 134.5, 133.7, 131.6, 131.2, 128.4, 126.1, 125.9, 125.6, 123.9, 123.6, 123.6, 123.5, 122.9, 121.6, 117.7, 54.1, 37.9. IR (KBr, /cm^{-1}): 3286, 3063, 2964,1641, 1551, 1451, 1345，1394，1309, 1251, 802, 797. Anal. Calcd for $C_{60}H_{57}N_{13}O_6$: C, 68.23; H, 5.44; N, 17.24. Found: C, 67.96; H, 5.71; N, 16.88. MS: *m/z* Calcd. for $[M+Cl]^-$, 1090.4237, found 1090.4435.

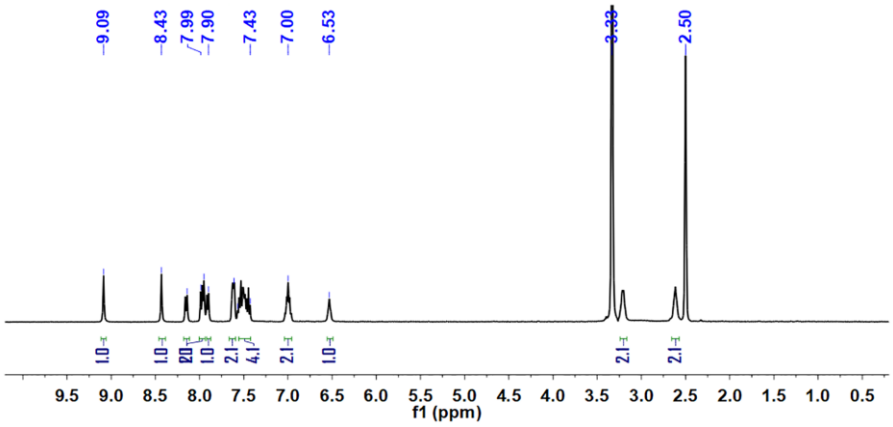

Fig. S1. ^{1}H NMR spectrum of ligand $\mathbf{L^2}$ (400 MHz, DMSO-d_6).

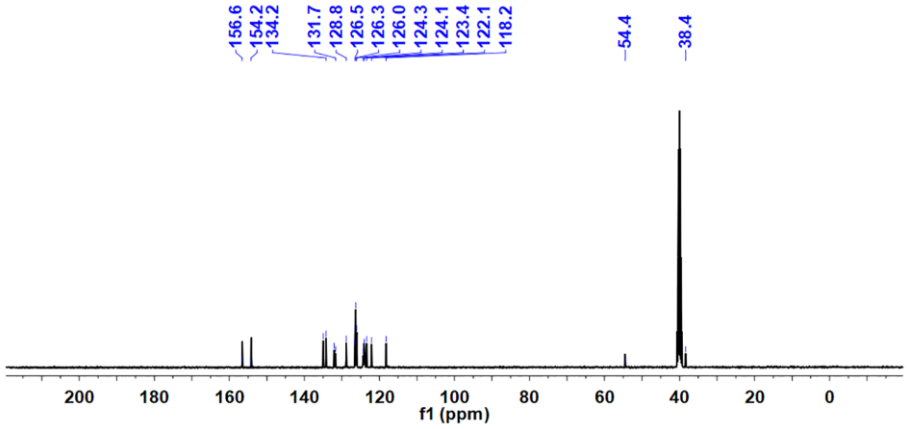

Fig. S2. ^{13}C NMR spectrum of compound $\mathbf{L^2}$ (100 MHz, DMSO-d_6).

Complex $Ch_2[L^2PO_4(Ch)]$ (1)

Ch_3PO_4 (1 mol/L, 20 uL, generated by choline hydroxide and H_3PO_4 in water) was added to a suspension of $\mathbf{L^2}$ (20 mg, 0.02 mmol) in acetonitrile (4 mL). After stirring overnight at room temperature, a clear colorless solution was obtained. Slow vapor diffusion of diethyl ether into this solution provided colorless crystals of complex $(Ch)_2[\mathbf{L^2}PO_4(Ch)_3]$ within three weeks. The identity of complex **1** was confirmed by HR MS (Fig. S6).

Complex (TBA)[L^1⊃CP] (2)

CP (0.25 mol/L, 80 uL, as TBA^+ salt generated by calcium phosphorylcholine chloride and (TBA)OH in water) was added to a suspension of $\mathbf{L^1}$ (20 mg, 0.02 mmol) in acetonitrile (4 mL). After stirring overnight at room temperature, a clear yellow solution was obtained. Slow vapor diffusion of diethyl ether into this solution provided yellow crystals of complex (TBA)[$\mathbf{L^1}$⊃CP] within two weeks. The identity of complex **2** was confirmed by HR MS (Fig. S7).

Complex (TMA)[L^2⊃CP] (3)

In a similar manner, treatment of $\mathbf{L^2}$ (20 mg, 0.02 mmol) with CP (0.25 mol/L, 80 uL, as TMA^+ salt) in acetonitrile (4 mL), followed by slow vapor diffusion of diethyl ether into the solution, provided colorless crystals of complex **3** within three weeks. The identity of **3** was confirmed by HR MS (Fig. S8).

S3. X-ray crystal structure analysis

X-ray diffraction data for complexes **1** and **3** were collected on a Bruker SMART APEX II diffractometer at 153 K with graphite-monochromated Mo Kα radiation (λ = 0.71073 Å). The diffraction data of complex **2** were collected on a Rigaku XtaLAB Pro diffractometer at 153 K with Cu-Kα radiation (λ = 1.54178 Å). An empirical absorption correction using SADABS was applied for all data. The structures of complexes **1**, **2** and **3** were solved by direct methods using the SHELXS-2014 program. All non-hydrogen atoms were refined anisotropically by full-matrix least-squares on F^2 by the use of the SHELXL program. Hydrogen atoms bonded to carbon and nitrogen atoms were included in idealized geometric positions with thermal parameters equivalent to 1.2 times those of the atom to which they were attached.

The remaining solvents could not be successfully resolved despite numerous attempts at modeling, and consequently the SQUEEZE function of PLATON was used to account for these highly disordered solvents. The removed void electron density corresponds to about 3.3 water molecules for complex **2** and 4.1 for complex **3**. The counter cations of complexes **1** and **2** were refined with restraints.

CCDC 1859609−1859611 contain the supplementary crystallographic data of complexes **1**−**3**. These data can be obtained free of charge from The Cambridge Crystallographic Data Centre via www.ccdc.cam.ac.uk/data_request/cif

Table S1. Crystal data and refinement details of complex **1**−**3**.

	complex **1**	complex **2**	complex **3**
Empirical formula	$C_{75}H_{99}N_{16}O_{13}P$	$C_{69}H_{97}N_{18}O_{16}P$	$C_{69}H_{82}N_{15}O_{10}P$
Formula weigtht	1462.73	1464.71	1311.61
Crystal System	Orthorhombic	Monoclinic	Triclinic
Space group	*Pna*2(1)	*P*2(1)/*n*	*P*-1
a (Å)	20.4627(5)	22.7938(8)	15.948(2)
b (Å)	15.7895(4)	18.9289(4)	16.487(2)
c (Å)	25.0638(6)	23.1163(8)	16.568(2)
α (deg)	90	90	98.9391(19)
β (deg)	90	119.257(5)	95.3315(18)
γ (deg)	90	90	117.1536(18)
V (Å^3)	8098.0(3)	8701.5(6)	3761.9(9)
Z	4	2	1
D_{calc}, g/cm^3	1.282	1.146	1.189
No. of unique data	18196	15239	12835
T (K)	153(2)	153(2)	153(2)
Total no. of data	80538	62489	24057
Crystal size (mm)	0.25 × 0.20 × 0.20	0.25 × 0.22 × 0.20	0.25 × 0.20 × 0.20
θ range	2.37−27.56	2.23−66.50	1.46−25.00
Completeness to θ	99.8 %	99.3%	96.9 %
R_{int}	0.0827	0.0401	0.0355
Goodness-of-fit-on F^2	1.144	1.044	1.020
R_1 [$I > 2\sigma(I)$]	0.0792	0.1074	0.0792
wR_2 [$I > 2\sigma(I)$]	0.1964	0.2146	0.1707

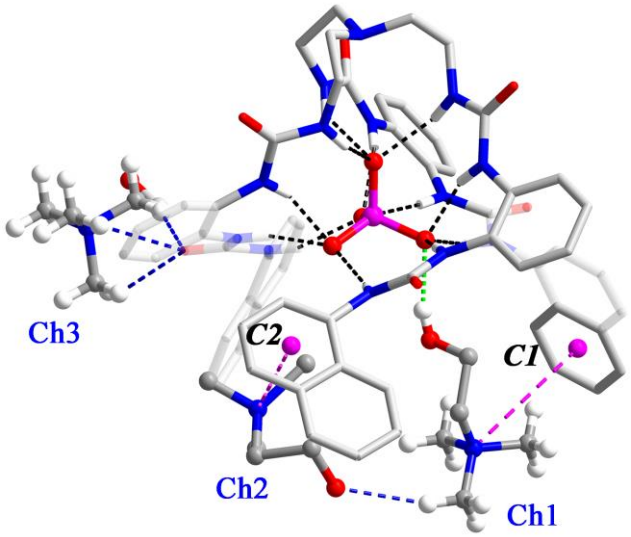

Fig. S3. Crystal structure of the ternary complex $[\mathbf{L}^{2}\bullet PO_4\bullet Ch]^{2-}$ showing the binding for the PO_4^{3-} anion and Ch^+ cation (Ch1) respectively, and interactions of the other two Ch^+ cations (Ch2 and Ch3), serving as counter ions, with the ligand. *C*1 and *C*2 represent centroids of aryl rings.

The Ch2 is located nearby and forms cation-π interactions with another naphthyl group (purple dashed line, N···*C*2 distance: 4.194 Å). The hydroxyl tail of Ch2 associates to Ch1 via a hydrogen bond (blue dashed line, C···O distance: 3.986 Å). The third choline ion (Ch3) is outside the tripodal cavity and the trimethylammonium head is bound with a urea carbonyl of the ligand via hydrogen bonds (blue dashed lines, C···O distances range from 3.179 to 3.468 Å, av. 3.298 Å).

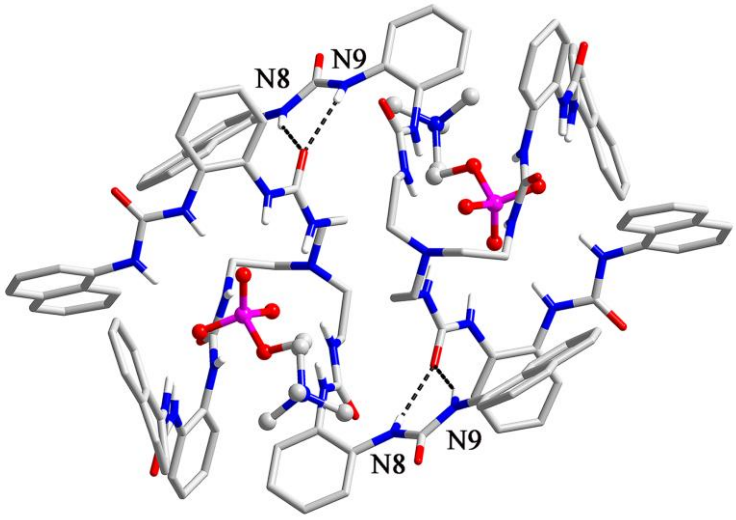

Fig. S4. A pair of symmetry-related urea···urea interactions dimerizes two $[\mathbf{L}^{2}\supset \mathbf{CP}]^{-}$ units.

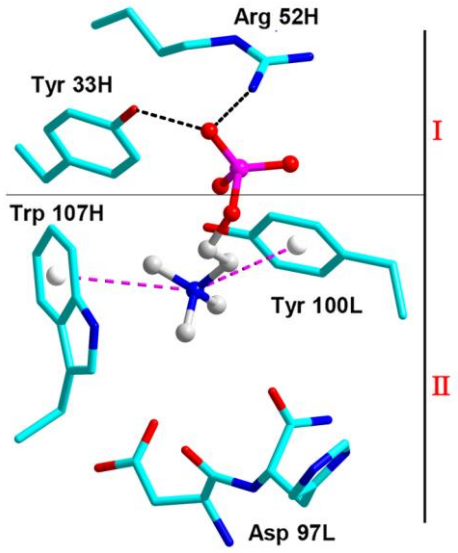

Fig. S5. Crystal structure of phosphocholine binding site of McPC603.[2] Tyr 33H (3.053 Å) and Arg 52H (2.922 Å) (site-I) provide hydrogen bonding for the phosphate group, while ion-ion (Asp97L) and cation-π interactions (Trp 107H, and Tyr 100L) (site-II) (4.158-4.505 Å) provide the binding affinity for the trimethylammonium group. Prepared using pymol (http://www.rcsb.org) and PDB ID: 2MCP.

Table S2. Hydrogen bond parameters [Å and °] in the crystal structure of complex Ch_2[$\mathbf{L}^2$·PO_4·Ch] (**1**).

D–H···A	d(D–H) (Å)	d(H···A) (Å)	d(D···A) (Å)	∠(DHA) (°)
N2–H2···O7	0.88	2.03	2.787(17)	143
N3–H3···O9	0.88	2.01	2.837(16)	156
N4–H4···O9	0.88	1.85	2.708(18)	164
N5–H5A···O10	0.88	1.95	2.764(18)	153
N6–H6A···O7	0.88	2.04	2.786(2)	142
N7–H7A···O8	0.88	2.19	3.038(19)	162
N8–H8A···O8	0.88	1.84	2.716(18)	173
N9–H9···O9	0.88	2.04	2.811(17)	146
N10–H10···O7	0.88	2.16	2.906(18)	142
N11–H11···O10	0.88	2.03	2.864(18)	158
N12–H12···O10	0.88	1.91	2.789(18)	173
N13–H13A···O8	0.88	1.93	2.754(19)	156

Table S3. Hydrogen bond parameters [Å and °] in the crystal structure of complex (TBA)**[L^1⊃CP]** (**2**).

D–H···A	d(D–H) (Å)	d(H···A) (Å)	d(D···A) (Å)	∠(DHA) (°)
N2–H2···O16	0.88	2.12	2.921(5)	152
N3–H3···O16	0.88	2.17	2.935(5)	145
N4–H4···O14	0.88	2.15	2.954 (5)	152
N5–H5A···O14	0.88	1.93	2.771(6)	158
N7–H7···O14	0.88	2.19	2.989(5)	151
N8–H8···O14	0.88	2.10	2.906(6)	152
N9–H9···O15	0.88	2.13	2.922(5)	149
N10–H10···O15	0.88	1.92	2.762(4)	158
N12–H12···O15	0.88	2.13	2.924(5)	150
N13–H13A···O15	0.88	2.04	2.844(6)	152
N14–H14···O16	0.88	2.27	3.053(6)	148
N15–H15A···O16	0.88	1.88	2.748(6)	166

Table S4. Hydrogen bond parameters [Å and °] in the crystal structure of complex (TMA)**[L^2⊃CP]** (**3**).

D–H···A	d(D–H) (Å)	d(H···A) (Å)	d(D···A) (Å)	∠(DHA) (°)
N2–H2···O7	0.88	2.19	3.029(4)	159
N3–H3···O9	0.88	1.91	2.768(4)	164
N4–H4···O9	0.88	1.86	2.736(5)	172
N5–H5···O8	0.88	2.25	3.075(5)	156
N6–H6···O7	0.88	2.29	3.019(4)	140
N7–H7···O7	0.88	2.26	2.937(4)	134
N10–H10···O7	0.88	2.19	2.942(4)	143
N11–H11···O8	0.88	2.38	3.151(4)	146
N12–H12A···O8	0.88	2.07	2.851(4)	148
N13–H13A···O8	0.88	2.10	2.893(4)	150

S4. Host-guest binding studies

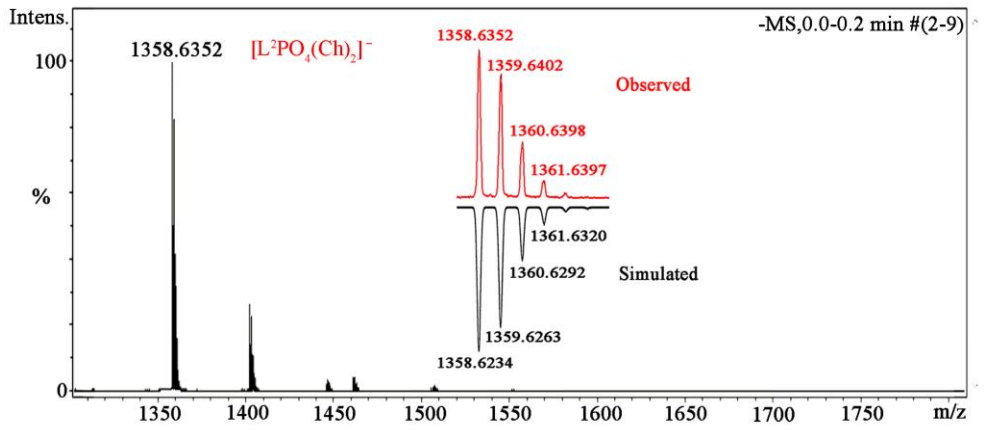

Fig. S6. High-resolution ESI-MS spectrum of complex $Ch_2[\mathbf{L}^{2}\cdot PO_4\cdot Ch]$ (**1**).

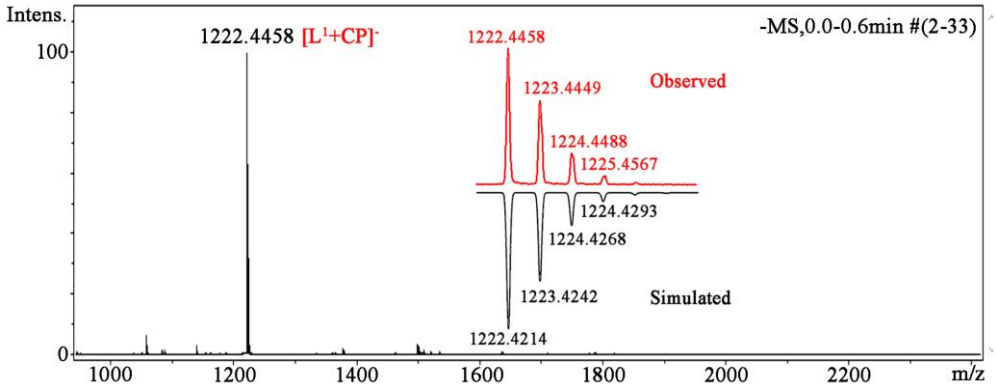

Fig. S7. High-resolution ESI-MS of complex (TBA)[$\mathbf{L}^{1}\supset$CP] **(2)**.

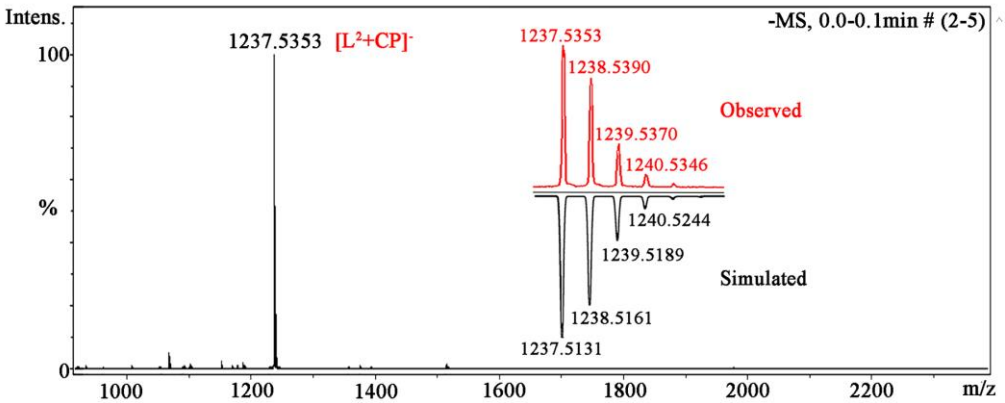

Fig. S8. High-resolution ESI-MS of (TMA)[$\mathbf{L}^{2}\supset$CP] (**3**).

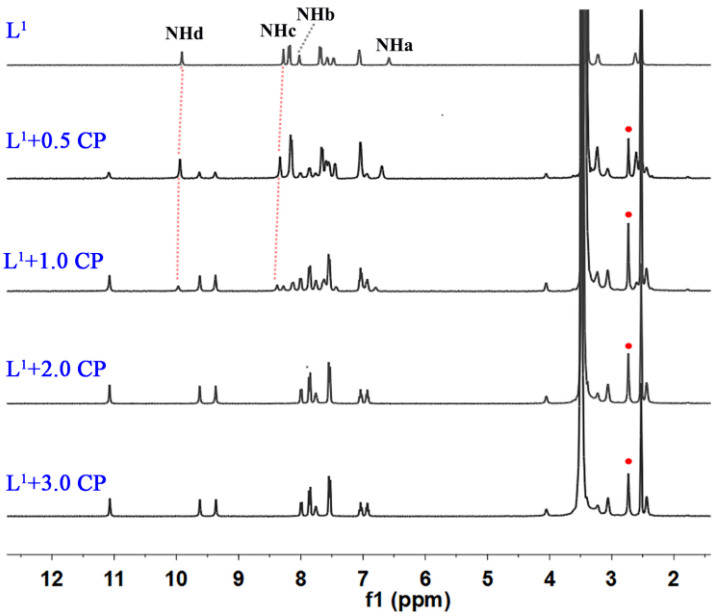

Fig. S9. ^{1}H NMR titration of **L^{1}** (2 mM) with CP (DMSO-d_6 /2% H_2O, 400 MHz).

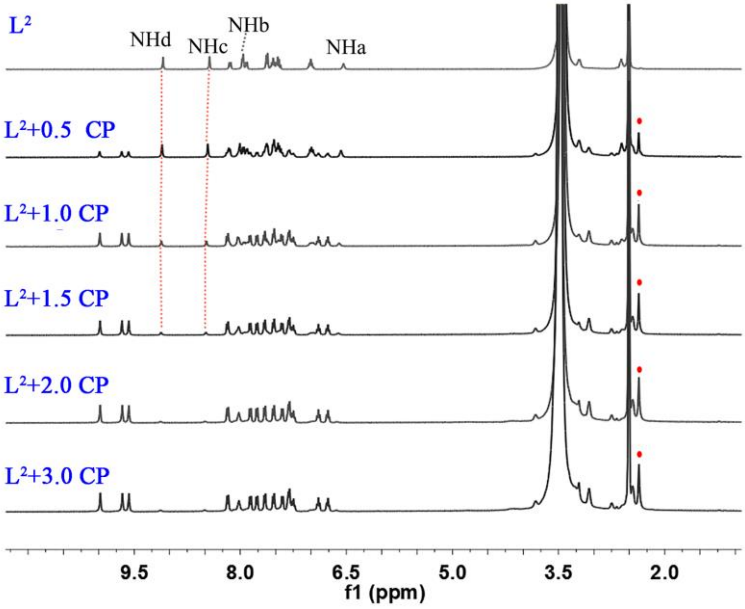

Fig. S10. ^{1}H NMR titration of **L^{2}** (2 mM) with CP (DMSO-d_6 /2% H_2O, 400 MHz).

Table S5. Change of the NH shifts (Δδ, ppm) of **L^{1}** + CP, **L^{2}** + CP, **L^{2}** + ADP and **L^{2}** + ATP.

	Δδ NHd	Δδ NHc	Δδ NHb	Δδ NHa	$\Delta\delta_{av}$
L^{1}+CP	1.18	1.10	1.61	1.17	1.27
L^{2}+CP	0.93	1.27	1.63	1.50	1.33
L^{2}+ADP	0.57	0.59	0.76	1.68	0.90
L^{2}+ATP	0.58	0.72	0.75	1.75	0.95

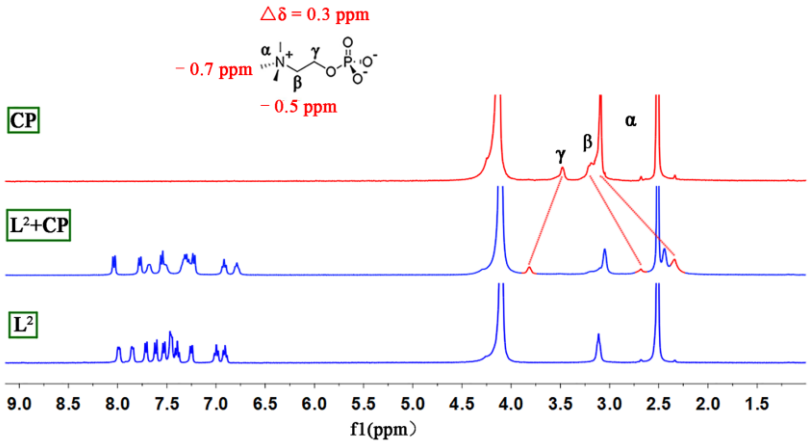

Fig. S11. Stacking ^{1}H NMR spectra (DMSO-d_6 /D_2O, v/v = 75/25, 400 MHz) of CP, $\mathbf{L}^{2}$ +1.0 equiv. CP, and $\mathbf{L}^{2}$ (2 mM).

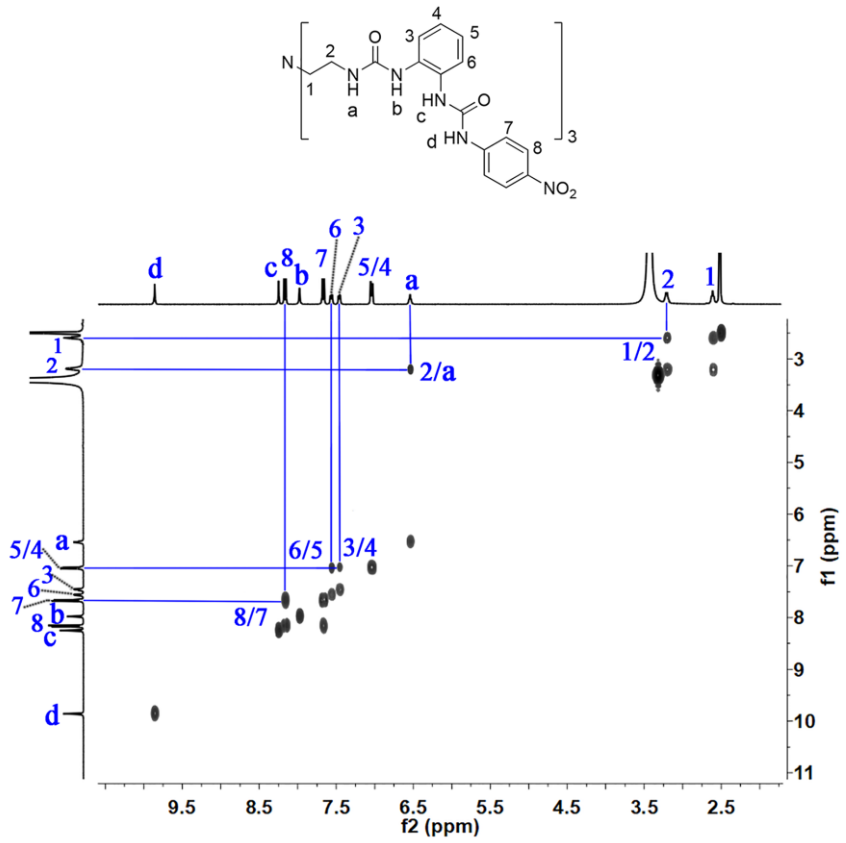

Fig. S12. Selected part of ^{1}H-^{1}H COSY spectrum (DMSO-d_6 /2% H_2O, 400 MHz) of $\mathbf{L}^{1}$.

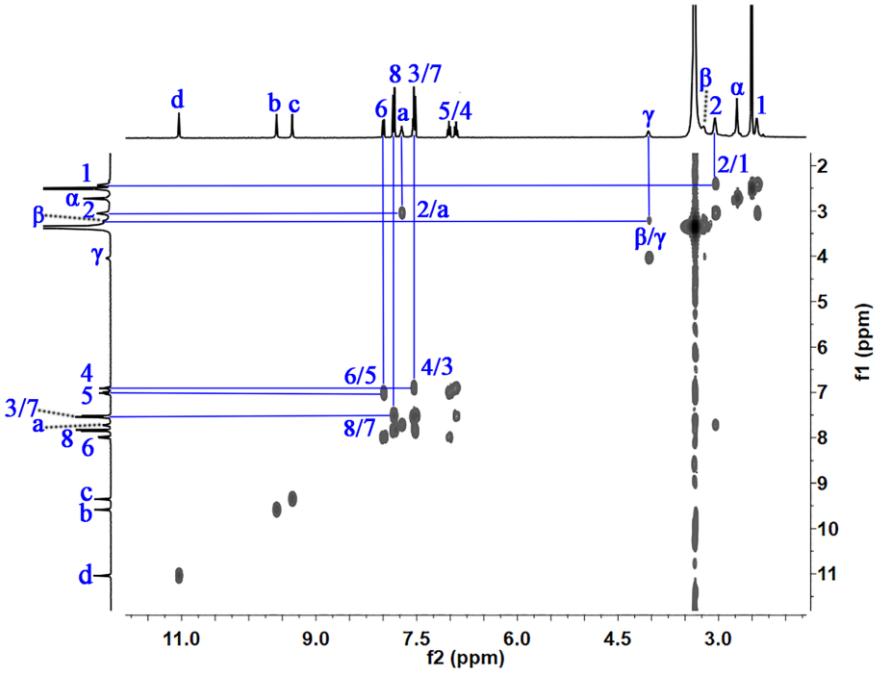

Fig. S13. Selected part of ^{1}H-^{1}H COSY spectrum (DMSO-d_6 /2% H_2O, 400 MHz) of $\mathbf{L}^{1}$+CP.

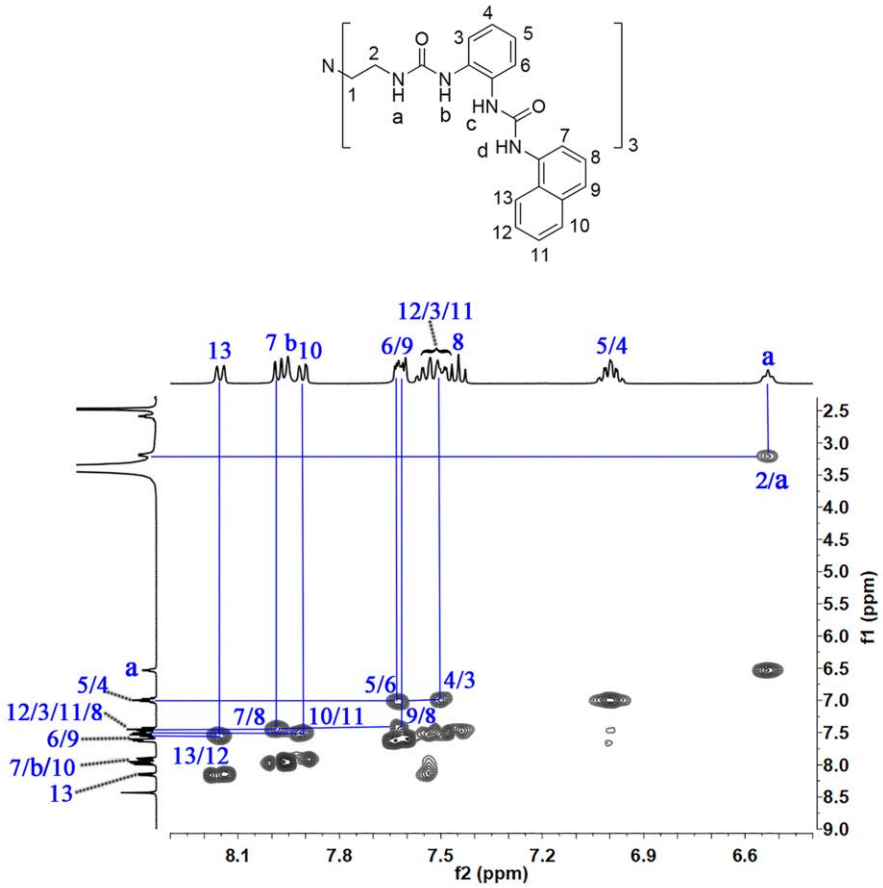

Fig. S14. Selected part of ^{1}H-^{1}H COSY spectrum (DMSO-d_6 /2% H_2O, 400 MHz) of $\mathbf{L}^{2}$.

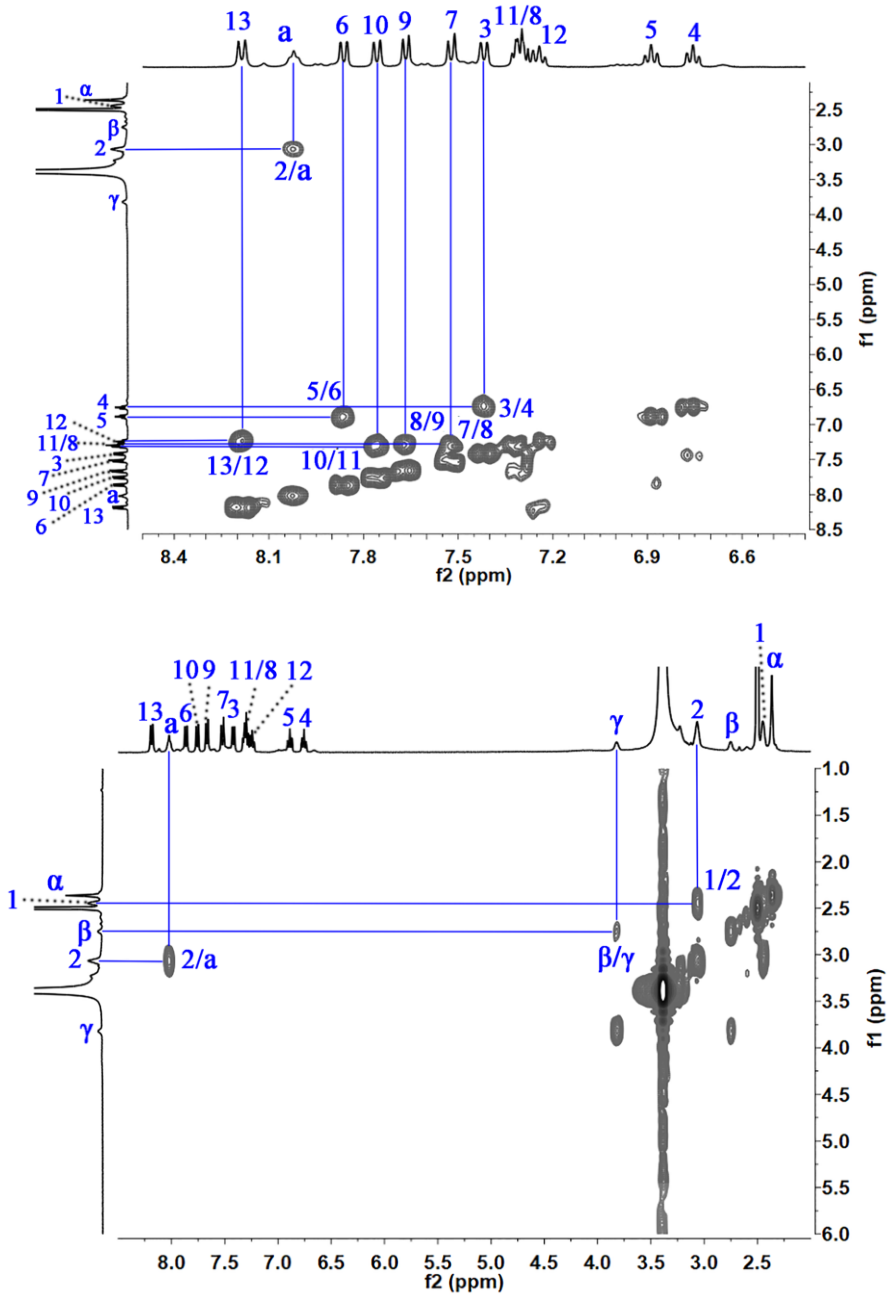

Fig. S15. Selected part of ^{1}H-^{1}H COSY spectrum (DMSO-d_6 /2% H_2O, 400 MHz) of $\mathbf{L}^2$+CP.

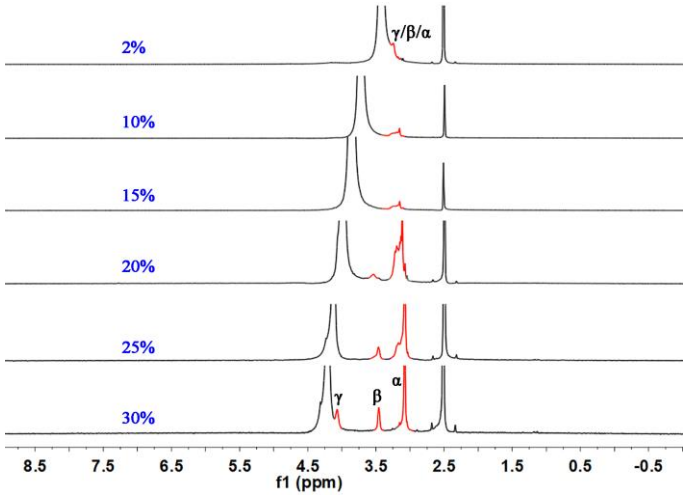

Fig. S16. ^{1}H NMR spectra of CP in different competitive solvents (DMSO-d_6 containing D_2O from 2% to 30%, 400 MHz).

S5. Fluorescence studies

All fluorescence titrations were performed at room temperature. Certain equivalents of a concentrated guest solution ([CP] = 1.0 mM or 10 mM; [ADP] = 10.0 mM, 0.5 M; [ATP] = 20.0 mM, 0.5M; [BP] = 2.0 mM, 5 mM, [DBP] = 10 mM, 0.1 M, [$HClO_4$] = 5 mM, [Ch] = [betaine] = [taurine] = [BTA] = 0.5 M) were added stepwise to a 3 mL solution of $\mathbf{L^2}$ in DMSO/H_2O (v/v = 98/2). As a very small volume of guest solution was added, the final amount of the solution was almost unchanged (3 mL). The mixed solution was incubated for 30 s and then irradiated at 310 nm. The corresponding emission intensities at 372 nm during titration were then recorded. Solutions of the host $\mathbf{L^2}$ and guest at the same concentration (10 μM) were prepared in DMSO containing 2% H_2O, used for determining the binding stoichiometry. Then the two solutions were mixed in different proportions maintaining a total volume of 3 mL and a total concentration of 10 μM. After incubating the mixture for 30 s, the spectra of the solutions for different compositions were recorded. The data was then collated and combined to produce data files from which so-called Job plots could be constructed.[3]

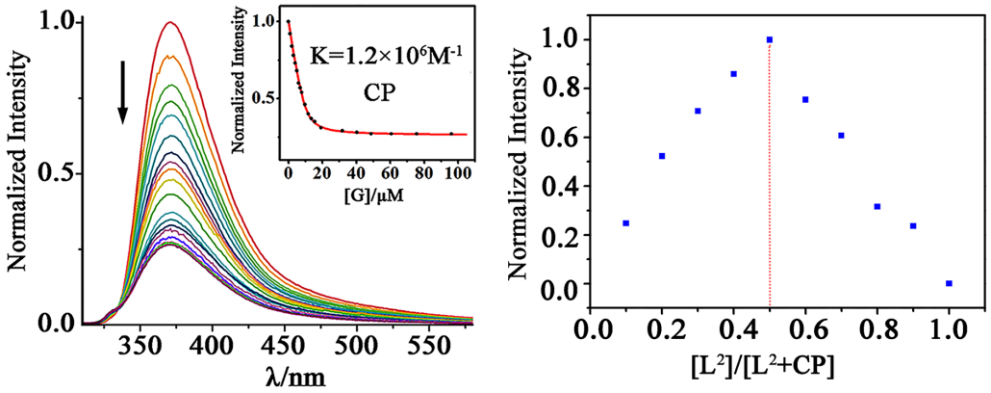

Fig. S17. Fluorescence titration of $\mathbf{L^2}$ (10 μM) with CP and Job's plot (DMSO/H_2O, v/v = 98/2).

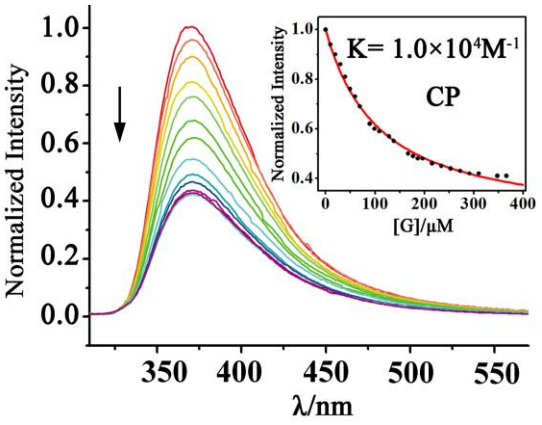

Fig. S18. Fluorescence titration of $\mathbf{L^2}$ (10 μM) with CP (DMSO/H_2O, v/v = 75/25).

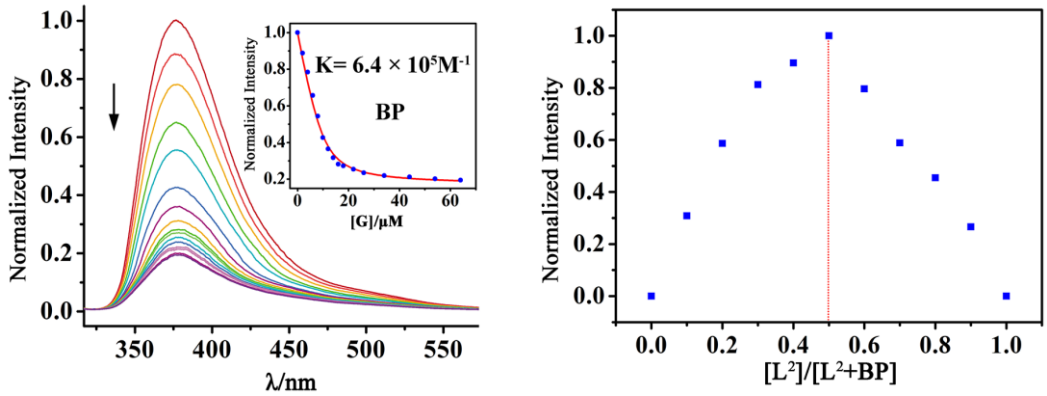

Fig. S19. Fluorescence titration of $\mathbf{L^2}$ (10 μM) with BP and Job's plot (DMSO/H_2O, v/v = 98/2).

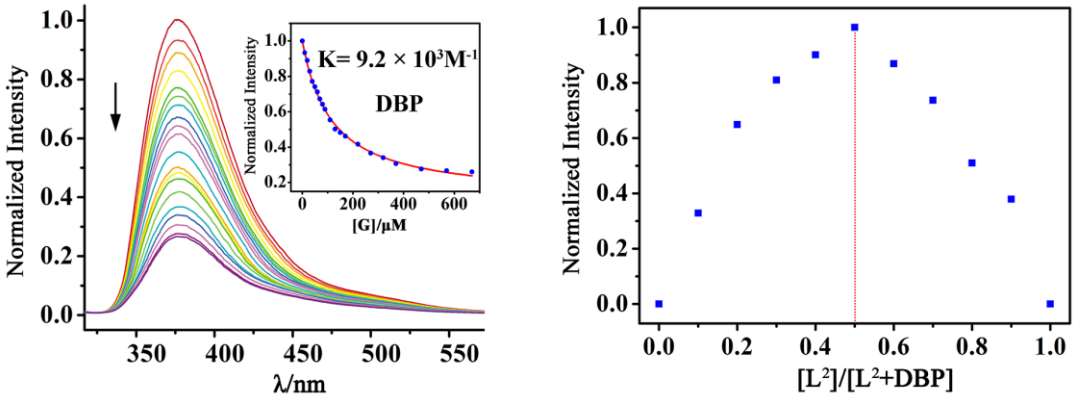

Fig. S20. Fluorescence titration of $\mathbf{L^2}$ (10 μM) with DBP and Job's plot (DMSO/H_2O, v/v = 98/2).

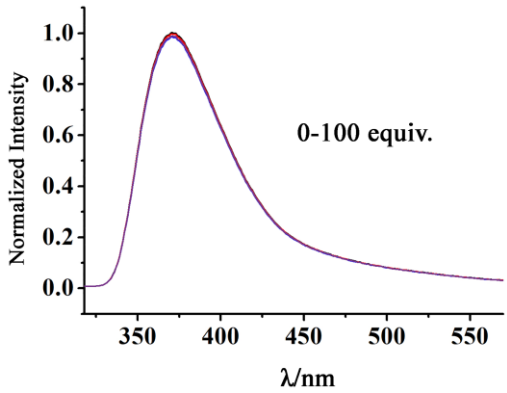

Fig. S21. Fluorescence titration of **L**^{2} (10 μM) with BTA (DMSO/H_2O, v/v = 98/2).

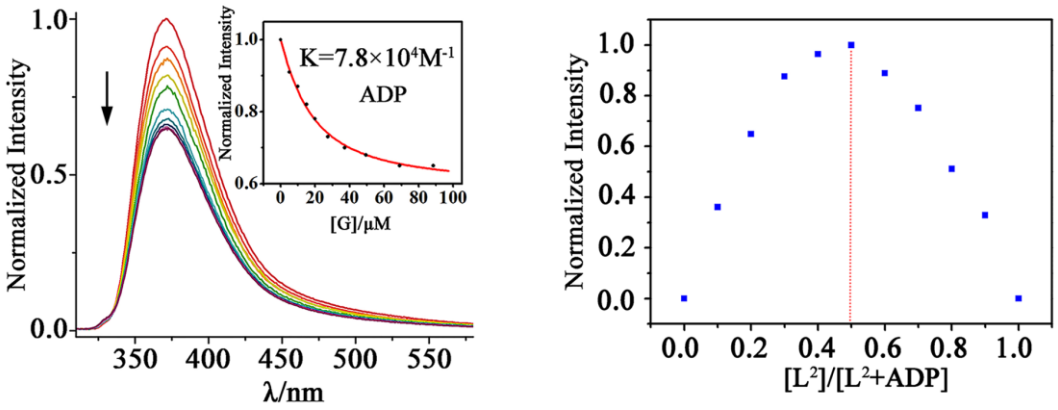

Fig. S22. Fluorescence titration of **L**^{2} (10 μM) with ADP and Job's plot (DMSO/H_2O, v/v = 98/2).

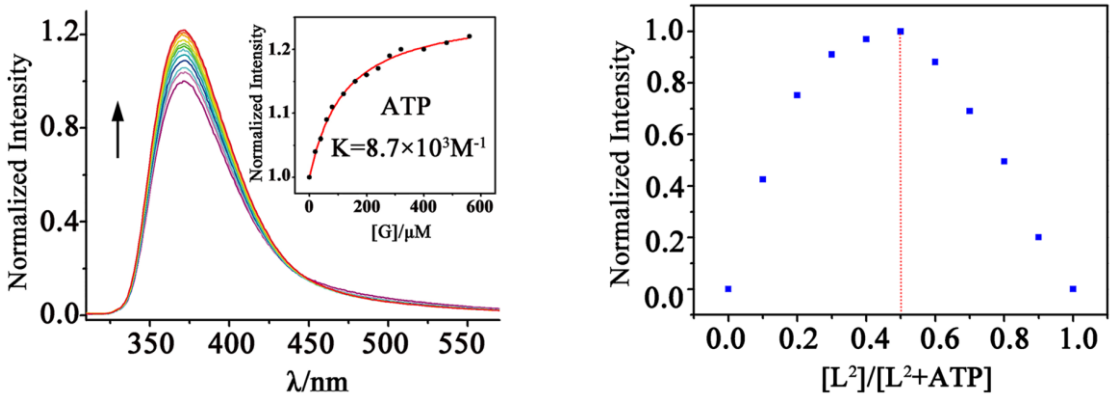

Fig. S23. Fluorescence titration of **L**^{2} (10 μM) with ATP and Job's plot (DMSO/H_2O, v/v = 98/2).

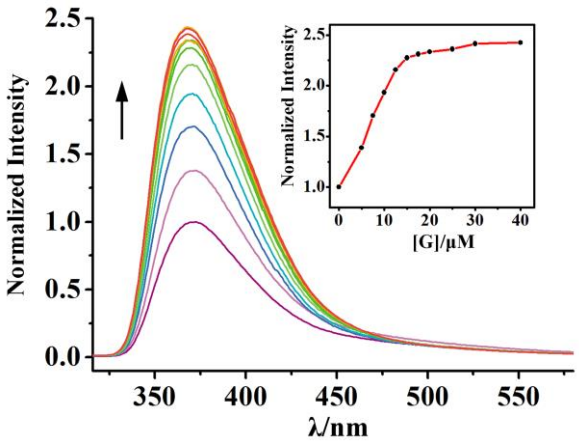

Fig. S24. Fluorescence titration of **L**^{2} (10 μM) with $HClO_4$ (DMSO/H_2O, v/v = 98/2).

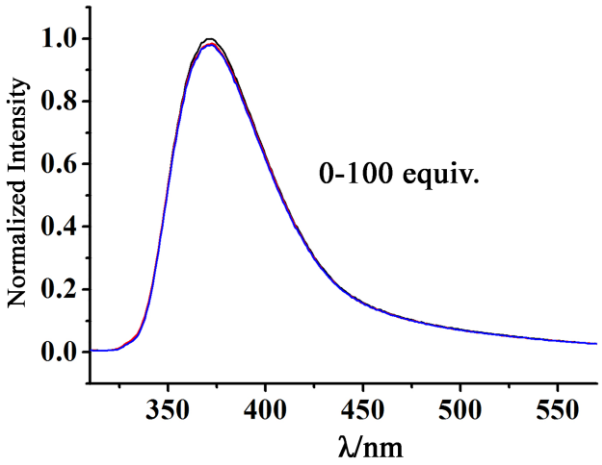

Fig. S25. Fluorescence titration of **L**^{2} (10 μM) with Ch (DMSO/H_2O, v/v = 98/2).

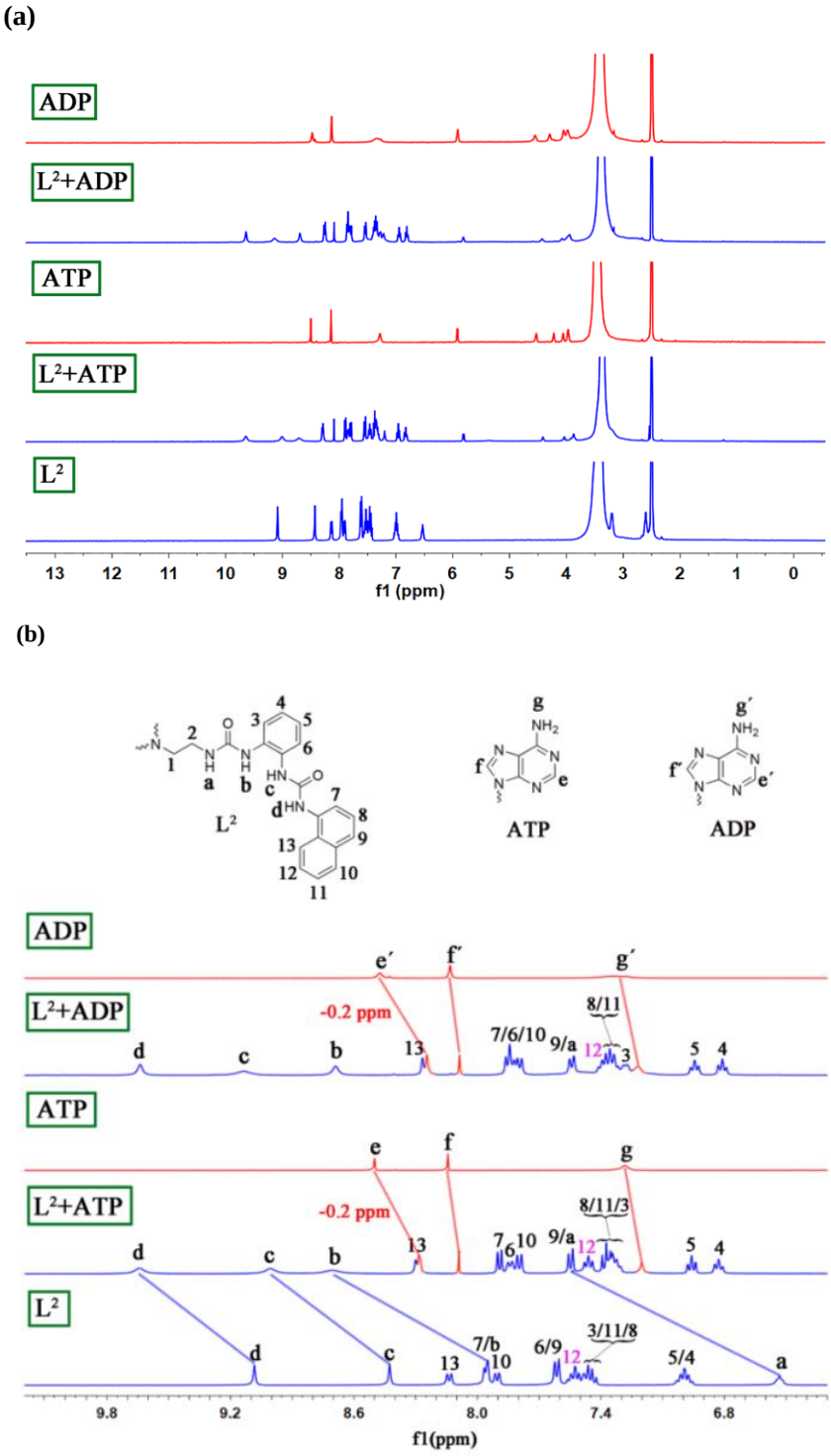

Fig. S26. (a) ^{1}H NMR spectra of $\mathbf{L^2}$ (2.0 mM) with 1.0 equiv of different guests (DMSO-d_6/2% H_2O, 400 MHz); (b) Enlarged partial ^{1}H NMR spectra of $\mathbf{L^2}$ (2 mM), $\mathbf{L^2}$ + ATP (1.0 equiv.), ATP, $\mathbf{L^2}$ + ADP (1.0 equiv.), and ADP.

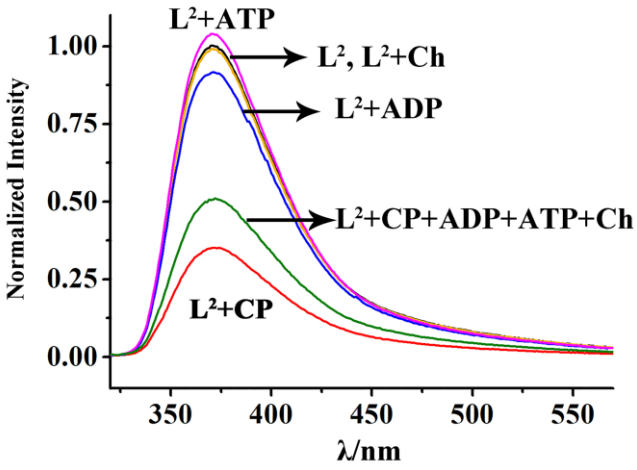

Fig. S27. Normalized spectra of $\mathbf{L^2}$ (10 μM) upon addition of 1.0 equiv. of different guests (DMSO/H_2O, v/v = 98/2).

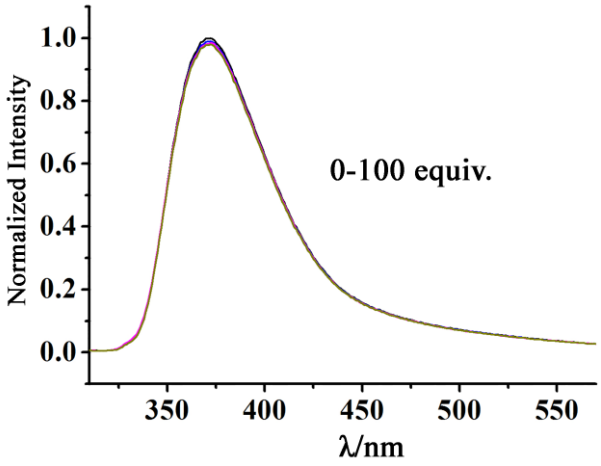

Fig. S28. Fluorescence titration of $\mathbf{L^2}$ (10 μM) with taurine (DMSO/H_2O, v/v = 98/2).

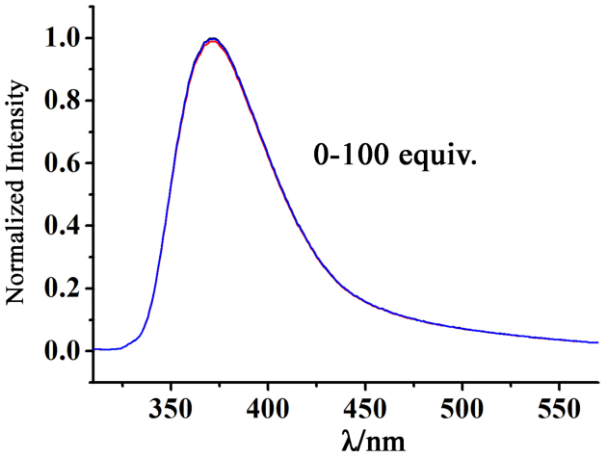

Fig. S29. Fluorescence titration of $\mathbf{L^2}$ (10 μM) with betaine (DMSO/H_2O, v/v = 98/2).

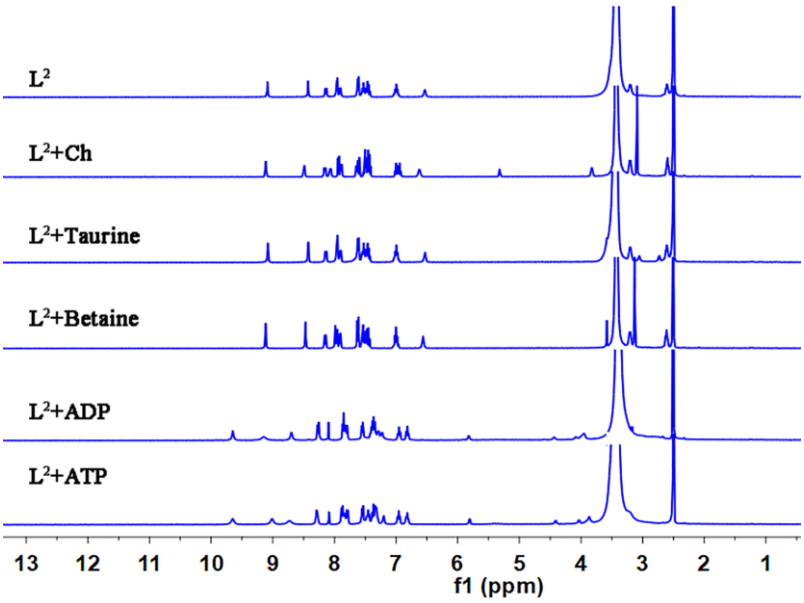

Fig. S30. ^{1}H NMR spectra of **L**^{2} (2.0 mM) with 1.0 equiv of different guests (DMSO-d_6 /2% H_2O, 400 MHz).

References

(1) C. Jia, B. Wu, S. Li, X. Huang, Q. Zhao, Q.-S. Li, X.-J. Yang, *Angew. Chem. Int. Ed.* **2011**, *50*, 486−490.

(2) E. A. Padlan, G. H. Cohen, D. R. Davies, PDB ID: 2MCP; unpublished work.

(3) J. L. Sessler, E. Katayev, G. D. Pantosa, Y. A. Ustynyuk, *Chem. Commun*. **2004**, 1276−1277.